[1]Ludwig-Maximilians-University Munich Klinikum Grosshadern, Radiation Oncology, Munich, Germany
[2]Ludwig-Maximilians-University Munich, Physics Department Medical Physics, Munich, Germany

Purpose/Objective: The sensitivity of QA protocols is tested for the novel Elekta Agility™ MLC (5 mm leaf width) and the widely used Elekta MLCi2 (10 mm leaf width) using both a 2D ionization chamber array (MatriXXevolution, iba dosimetry) and a 2D diode array (MapCHECK 2, Sun Nuclear).
Materials and Methods: Geometric characterisation includes detection of leaf and jaw penumbra as well as detection of leaf misalignments using a 'comb field' with shifts of adjacent leaves ranging from 1 to 5 mm. Further accuracy checks are done evaluating tongue-and-grove,stair pattern and picket fence test. These fields are measured in original setup position and with the devices shifted half a leaf towards the gantry. Results are compared against EBT3 film and Monte Carlo dose calculations. Dosimetric accuracy is checked against a Farmer-type ionisation chamber (FC) with respect to dose linearity and dose summation.
Results: Dose linearity and dose summation for MatriXX is always consistent (<0.5 %) with the FC. MapCHECK shows consistency (<0.5 %) for doses higher than 15 cGy. Smaller doses (2 cGy) are measured with up to -3 % deviation. Penumbras measured with MapCHECK are consistent with film measurements. Depending on the steepness of the penumbra, MatriXX shows up to 2.8 mm wider penumbras. Measurements of the comb field show that both devices detect leaf misalignments down to 1mm. However, the amount of the dose perturbation is highly dependent on the geometry of the misaligned leaf relative to the detector geometry, especially for the smaller leaf widths of the Agility MLC (5 mm). Accuracy checks show higher sensitivity of leaf misalignments for MapCHECK. Combining original and shifted measurements, MatriXX provides the same information.
Conclusions: Both arrays are suitable for 2D dose measurements, even though every device has specific strengths. MatriXX performes better for dose linearity and dose summation due to the use of ionization chambers. MapCHECK is advantageous in MLC accuracy measurements due to the detector geometry setup and the point-like detection characteristics of diode detectors. Using either array with MLCi2 (10 mm), each device will provide sufficient measurements for patient specific QA using a Gamma Index 3% / 3mm. However, the smaller the leaves the better MapCHECK will detect leaf misalignments. MatriXX performs better if many subfields have small MU. Using the devices for machine QA, it is highly important to design tests in accordance to the measurement geometry. Especially for MatriXX measurements with small MLCs (e.g. Agility) measurements of original and shifted setups need to be combined for sufficient MLC QA.

PD-0569

Incorporating dynamic motion in PENELOPE

C. Le Loirec[1], B. Poumarede[1], E. Barat[1], T. Dautremer[1], T. Montagu[1], L. Guerin[2], A. Batalla[2], D. Lazaro[1]
[1]*CEA Saclay, DRT/LIST, Gif sur Yvette, France*
[2]*Centre F. Baclesse, Physics, Caen, France*

Purpose/Objective: The traditional way to take time into account in Monte Carlo (MC) simulations is to simulate individual static component fields separately and integrate the results. This method can be very efficient but leads to a high demand of phase space file storage. To avoid this, the position probability sampling (PPS) method, in which the position of a geometrical object is treated as a random variable during the simulation, has been developed. We aim here to incorporate this method in Penelope in the case of a virtual wedge.
Materials and Methods
II.1 Monte Carlo simulation: We have used the 2006 release of the Penelope code with a new version of the main program Penmain, in which several conventional variance reduction techniques were implemented in order to increase the efficiency of the linac treatment head simulations. The MC code was used to model both the Siemens Artiste linac with a full description of the Siemens 160 MLC and the OptiVue™ 1000 EPID (Siemens Medical Solutions).
To model the dynamic jaw motion of the virtual wedge, the PPS method has been implemented in Penmain. This implementation required an adequate modelling of the jaws to allow their motion without a complete re-initialization of the geometry for each particle. We have thus written a new subroutine which needs as inputs: the index of the moving jaw surface, the first and last positions of the moving jaw, the wedge angle a, and the value of (C x μ) with μ the effective linear attenuation coefficient in water for the particular photon spectrum, and C a tuning coefficient for μ.
II.2 Measurements
All the measurements have been performed on a Siemens Artiste linac with a 20 cm x 20 cm field size and for a 6 MV photon beam. A first set of measurements has been performed in a water tank positioned at 100 cm skin source distance. Wedged beam profiles have been measured with a linear detector array at three different depths: 1.5 cm, 5 cm, and 10 cm. Then a portal image of a 40° wedged beam has been acquired at 145 cm detector source distance without any phantom in the beam.
Results: We have first performed MC simulations for the 45° wedged beam in a water tank and we have reported the dose distribution in a 4 x 3 x 2.5 mm^3 scoring grid. The profiles have been extracted and compared with the experimental ones. We have then simulated the acquisition of the portal image of a 45° wedged beam with the EPID's physical resolution (0.39 mm). The results are reported in figure 1.

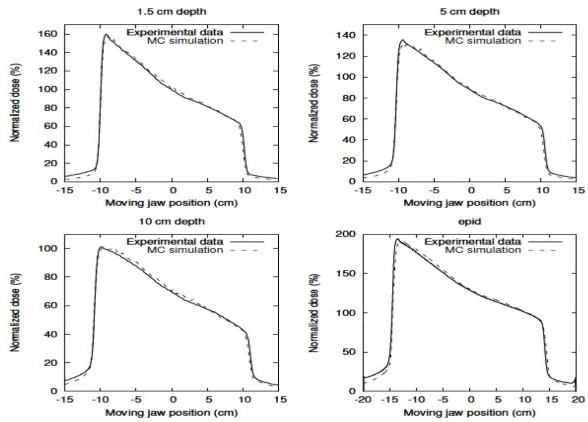

Conclusions: In this work the PPS method was used to incorporate the collimator motion into Penelope. A 6 MV photon beam of a Siemens Artiste linac equipped with a 160 MLC and an OptiVue™ 1000 EPID (Siemens Medical Solutions) was simulated with a virtual wedge. Measurements and simulations have been performed in a water tank and in the portal device. The simulated dose profiles reproduce the experimental data with a fairly good accuracy.

PD-0570

A comparison of the beam configuration modules of two proton treatment planning systems.

P. Doolan[1], I. Rosenberg[2], C. Ainsley[3], A. Gibson[1], G. Royle[1]
[1]*University College London, Department of Medical Physics and Bioengineering, London, United Kingdom*
[2]*University College London Hospital, Department of Radiotherapy, London, United Kingdom*
[3]*University of Pennsylvania, Department of Radiation Oncology, Philadelphia, USA*

Purpose/Objective: With the potential improvement of dose conformality of protons over photons, the number of new proton treatment centres is increasing rapidly. One of the key physics decisions for a new centre is the choice of treatment planning system and one of the first important tasks facing the physics team is beam commissioning. Proton beam commissioning consists of modelling pristine Bragg peaks and lateral profiles for the range of energies to be used clinically. Both are equally important as they effectively define the proximal/distal and lateral beam penumbrae respectively. This study analyses the performance of beam configuration modules of two treatment planning systems: commercially-available Eclipse (v10.0.39) and research-only Pinnacle (v9.1, Feb 2012).
Materials and Methods: Pristine Bragg peaks (for 27 energies between 100-226.7MeV) from the University of Pennsylvania horizontal fixed beam line were acquired in a water tank with a 42mm measurement offset (water tank wall, surface offset and chamber offset). Lateral profiles were acquired at 8 positions in air, for each energy, using IBA's Lynx scintillator/CCD camera system. The depth dose curves and profiles were modelled by both systems using their respective automated fitting tools. After resampling the measured and fitted datasets to a consistent high resolution, the fitting quality was assessed using gamma analysis with a 2%/2mm criteria for depth dose curves and a 2%/0.1mm criteria for lateral profiles. The tighter distance-to-agreement criterion was required for profiles to ensure the analysis did not reach a false local minimum.
Results: Both models were within clinical tolerances, however their algorithms differ and so there were slight differences in the fitting. For energies E>180MeV in Eclipse the entrance dose in the depth dose curves was underestimated (by up to 2.5%), while Pinnacle consistently overestimates the distal Bragg peak depth with a mean distal R50 error of 0.3mm. The mean gamma index for the profiles,

across the 8 measurement positions, is small and similar for both systems (both <0.25). In the y-direction the mean gamma index is similar for both systems and decreases with increasing energy, but is always less than 0.5.

Conclusions: Both systems produce beam models within clinically-accepted tolerances however the differences in algorithms lead to minor fitting differences. Perhaps the most important difference is Pinnacle's consistent overestimation of the Bragg peak depth (0.3mm on average). It should be noted however that this problem has since been addressed in the latest Pinnacle update (July 2012), to allow an increased weighting to be placed on the distal edge during the fitting process. It would be of interest to investigate how the fitting errors translate to benchmarking in a phantom.

PD-0571

Is the TPS photon field implementation detector-depending?

M. Fortunato[1], P. Colleoni[1], S. Andreoli[1], M. Di Martino[1], R. Moretti[1]
[1]*Ospedali Riuniti di Bergamo, USC Fisica Sanitaria, Bergamo, Italy*

Purpose/Objective: The dosimetric characterization of a photon field can show relevant differences depending on the used detectors. The focus of this work is to evaluate the influence of these differences in Treatment Planning System (TPS) algorithm, implementing different machines (each one for every detector, i.e. 'detector-machine'). Validated the reliability of the algorithm for our reference detector-machine by the IAEA TECDOC 1540 and 1583, the comparison among the detector-machines could be made for different plans in water, slab antropomorphic phantom and on clinical CT images by the $\Gamma(\delta x,\delta d)$ function.

Materials and Methods: A 6MV photon field (Varian Clinac 6EX) was implemented with Varian Eclipse AAA algorithm (v.10.0.28). The Dose Profiles, the Percentual Depth Dose and the Output Factors (open fields, 2x2 to 40x40 cm) have been measured for each detector-machine. The different machines were obtained with the following PTW detectors: µLion, semiflex 0.125, unshielded diode and diamond. The µLion-machine has been chosen as reference after being validated with IAEA TECDOC 1540 and 1583 tests in water and in slab phantom (Easy-Cube, Euromechanics) by a semiflex 0.125 chamber for dose point calculation. Then the $\Gamma(\delta x,\delta d)$ function was evaluated matching fourteen plan dose matrices extracted from the TPS for different plans studied with each detector-machine in water, in the slab phantom and by plans based on clinical TC images for the breast, lung and pelvis districts. Two dose deviation/error position criteria have been considered: 3%/1mm (TPS calculation grid) and 1%/0,1mm. Because the dose matrices were calculated on the same TC images, the positional error Δx in $\Gamma(\delta x,\delta d)$ function can be considered null, so $\Gamma(\delta x,\delta d) = \Gamma(\delta d)$.

Results: The IAEA validation tests shown that the µLion-machine was in good agreement with the dose tolerance recommended value. Among the fourteen plan dose matrices, in table are presented the worst case comparison between machines (respect to µLion-machine).

	Criteria	
Detector	3% , 1mm	1% , 0.1mm
semiflex 0.125	0.2 %	6.0 %
unshielded diode	1.7 %	27.6 %
diamond	34.2 %	74.7 %

Conclusions: In relative field characterization, substantial differences were observed at the edges profiles and for points at pre-buildup and over 30 cm dephts. The 3%/1mm criteria shows no significant differences, while the second one emphasizes coincidences between the two ion chambers (semiflex and µLion). There are evidence of differences in calculated dose in anatomical regions with high gradient density (see the attached figure where the comparison between µLion and unshielded diode detector-machine for a 10x10cm field is shown), but negligible considering the criteria of comparison. Experimental verification with detector arrays (MapCheck and ArcCheck SNC) are in progress.

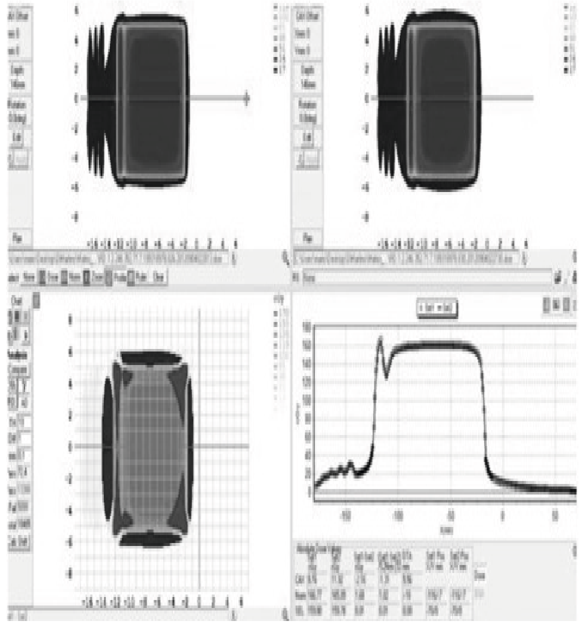

POSTER DISCUSSION: YOUNG SCIENTISTS 7: IMAGE REGISTRATION AND MANAGEMENT OF INTRA- AND INTERFRACTION MOTION

PD-0572

Physical validation of a deformable CT-CBCT registration tool for IGRT

L. Boldrini[1], L. Placidi[2], G.C. Mattiucci[1], G.R. D'Agostino[1], D. Raspanti[3], V. Valentini[1], A. Fidanzio[2]
[1]*Università Cattolica del Sacro Cuore, Radiation Oncology, Rome, Italy*
[2]*Università Cattolica del Sacro Cuore, Medical Physics, Rome, Italy*
[3]*Tema Sinergie, Faenza, Italy*

Purpose/Objective: Deformable registrations between simulation CT and CBCT images were performed by the MIM 5.5.2 software in order to assess its capability in accounting for organ movement and morphologic variations.

Materials and Methods: Two phantoms were realized with different density inserts and a fixed structure (to simulate bone structures). Two different configurations for each phantom were designed: the first one was acquired only by CT scanner, the second one, with modified dimensions and positions of the insert, was acquired by CT scanner and three CBCT image acquisition protocols (high, medium and low definition: HD, MD, LD). In the second phantom configuration, the volumes of the insert were reduced between 20% and 60% and its geometric positions were changed within 1 cm. All the structures were contoured. Deformable registrations were performed by MIM 5.5.2 software, obtaining surrogate images with autocontoured inserts. In particular for each phantom the first configuration CT images were deformed on the CT and CBCT images of the second configuration. Volume differences, HU differences, centroid's coordinates difference, Pearson coefficients and Dice Similarity Index (DSI) were determined between the surrogates and the images of the second configuration phantoms, to assess the fusion algorithm.

Results: For the surrogates obtained by the registration of the CT images of the two phantom configurations, Pearson correlation coefficient equal to 0.996, insert volume variations within 2%, mean insert HU variations within 1.5%, centroid's coordinate variations within 1mm and DSI values equal to 0.99, were observed. Regarding the surrogate obtained by the deformable registration of the CT with the different CBCT resolutions (high, medium and low), we observed Pearson coefficient correlation variation from 0.997 to 0.995, insert volume variations range between 6% and 8%, mean insert HU range from 5% to 9%. The centroid's coordinate variations are within 1mm and the Dice values changes between 0.91-0.97. (Tab.1)